Bull. Korean Math. Soc. **56** (2019), No. 1, pp. 265–276
https://doi.org/10.4134/BKMS.b180238
pISSN: 1015-8634 / eISSN: 2234-3016

A NONLINEAR CONVEX SPLITTING FOURIER SPECTRAL SCHEME FOR THE CAHN–HILLIARD EQUATION WITH A LOGARITHMIC FREE ENERGY

Junseok Kim and Hyun Geun Lee

Reprinted from the
Bulletin of the Korean Mathematical Society
Vol. 56, No. 1, January 2019

Bull. Korean Math. Soc. **56** (2019), No. 1, pp. 265–276
https://doi.org/10.4134/BKMS.b180238
pISSN: 1015-8634 / eISSN: 2234-3016

A NONLINEAR CONVEX SPLITTING FOURIER SPECTRAL SCHEME FOR THE CAHN–HILLIARD EQUATION WITH A LOGARITHMIC FREE ENERGY

Junseok Kim and Hyun Geun Lee

Abstract. For a simple implementation, a linear convex splitting scheme was coupled with the Fourier spectral method for the Cahn–Hilliard equation with a logarithmic free energy. However, an inappropriate value of the splitting parameter of the linear scheme may lead to incorrect morphologies in the phase separation process. In order to overcome this problem, we present a nonlinear convex splitting Fourier spectral scheme for the Cahn–Hilliard equation with a logarithmic free energy, which is an appropriate extension of Eyre's idea of convex-concave decomposition of the energy functional. Using the nonlinear scheme, we derive a useful formula for the relation between the gradient energy coefficient and the thickness of the interfacial layer. And we present numerical simulations showing the different evolution of the solution using the linear and nonlinear schemes. The numerical results demonstrate that the nonlinear scheme is more accurate than the linear one.

1. Introduction

When a homogeneous system at high temperature is quenched to an absolute temperature θ below a critical temperature θ_c, phase separation takes place [2, 3]. Figure 1 shows the evolution of spinodal morphology as seen by atomic force microscopy topography of the microtomed films [1].

This phenomenon can be modeled by the Cahn–Hilliard (CH) equation with a logarithmic free energy [2, 3]:

$$\frac{\partial \phi}{\partial t} = \Delta \left[\frac{\theta}{2} \ln \left(\frac{1+\phi}{1-\phi} \right) - \theta_c \phi - \epsilon^2 \Delta \phi \right], \quad \mathbf{x} \in \Omega,\ 0 < t \le T, \tag{1}$$

Received March 16, 2018; Revised July 10, 2018; Accepted October 11, 2018.
2010 *Mathematics Subject Classification.* 35Q99, 65M70.
Key words and phrases. nonlinear convex splitting scheme, Fourier spectral method, Cahn–Hilliard equation, logarithmic free energy, phase separation.
J. S. Kim was supported by Korea University Future Research Grant. H. G. Lee was supported by Basic Science Research Program through the National Research Foundation of Korea (NRF) funded by the Ministry of Education (2017R1D1A1B03034619).

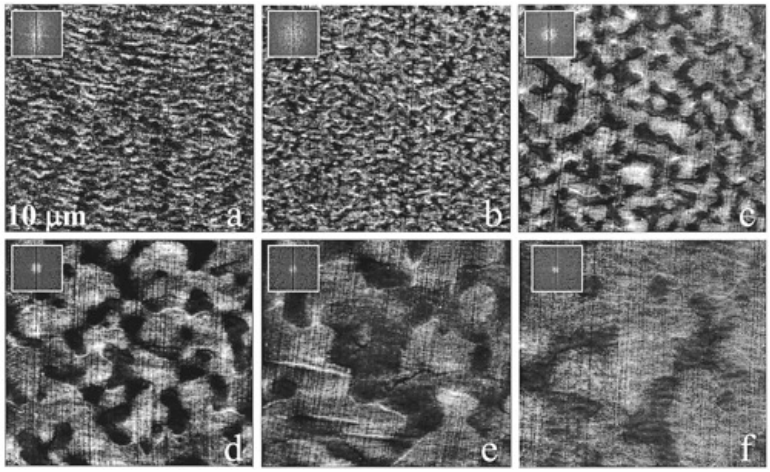

FIGURE 1. Spinodal decomposition kinetics of polycarbonate and polystyrene 50 : 50 at various times: (a) 50, (b) 100, (c) 300, (d) 500, (e) 700, and (f) 1000s. Reprinted with permission from [1]. Copyright (2001) American Chemical Society.

where ϕ is the difference between the concentrations of the two components in a mixture, $\epsilon > 0$ is the gradient energy coefficient, Ω is a domain in $\mathbb{R}^d$ $(d = 1, 2, 3)$, and T is a final time. The CH equation (1) is derived from the Ginzburg–Landau free energy functional:

$$\mathcal{E}(\phi) := \int_\Omega \left(F(\phi) + \frac{\epsilon^2}{2} |\nabla \phi|^2 \right) d\mathbf{x}, \tag{2}$$

where the logarithmic free energy $F(\phi)$ is given by

$$F(\phi) = \frac{\theta}{2} \left[(1+\phi) \ln \left(\frac{1+\phi}{2} \right) + (1-\phi) \ln \left(\frac{1-\phi}{2} \right) \right] + \frac{\theta_c}{2} (1 - \phi^2). \tag{3}$$

See the review paper [13] for the physical, mathematical, and numerical derivations for the CH equation.

The CH equation is a fourth-order nonlinear partial differential equation and cannot generally be solved analytically, thus, numerical methods are commonly used to study the dynamics of the CH equation. For the spatial discretization, finite difference [10, 16, 18], finite element [7, 9], and Fourier spectral [4, 5, 17] methods were used. Here, we employ the Fourier spectral method for the spatial discretization. For a simple implementation, a linear convex splitting scheme was coupled with the Fourier spectral method for the CH equation in [11]. However, we observe through numerical simulations that an inappropriate value of the splitting parameter of the linear scheme may lead to incorrect

morphologies in the phase separation process. In order to overcome this problem, we present a nonlinear convex splitting Fourier spectral scheme for the CH equation with a logarithmic free energy, which is an appropriate extension of Eyre's idea of convex-concave decomposition of the energy functional with a polynomial free energy [8].

This paper is organized as follows. In Section 2, we describe the nonlinear scheme for the CH equation with a logarithmic free energy. In Section 3, we derive a useful formula for the relation between the ϵ value and the thickness of the interfacial layer using the nonlinear scheme. And we briefly describe a linear convex splitting scheme and present numerical simulations showing the different evolution of the solution using the linear and nonlinear schemes. Finally, conclusions are drawn in Section 4.

2. Numerical solution

We consider the CH equation (1) in two-dimensional periodic space $\Omega = [0, L_1] \times [0, L_2]$ for simplicity of description. Let N_1 and N_2 be positive integers, $h = L_1/N_1 = L_2/N_2$ be the space step size, and Δt be the time step size. Let $\phi^n_{l_1 l_2}$ be an approximation of $\phi(x_{l_1}, y_{l_2}, t^n)$, where $x_{l_1} = l_1 h$ for $l_1 = 0, 1, \ldots, N_1 - 1$, $y_{l_2} = l_2 h$ for $l_2 = 0, 1, \ldots, N_2 - 1$, and $t^n = n\Delta t$. In order to solve Eq. (1) with the periodic boundary condition, we employ the discrete Fourier transform: for $k_1 = 0, 1, \ldots, N_1 - 1$, $k_2 = 0, 1, \ldots, N_2 - 1$, $\widehat{\phi}_{k_1 k_2} = \sum_{l_1=0}^{N_1-1} \sum_{l_2=0}^{N_2-1} \phi_{l_1 l_2} e^{-i\left(x_{l_1}\xi_{k_1} + y_{l_2}\xi_{k_2}\right)}$, where $\xi_{k_1} = 2\pi k_1/L_1$ and $\xi_{k_2} = 2\pi k_2/L_2$.

A nonlinear convex splitting scheme for Eq. (1) is based on the observation that the energy functional $\mathcal{E}(\phi)$ in (2) can be split into convex and concave parts:

$$\mathcal{E}(\phi) = \mathcal{E}_c(\phi) - \mathcal{E}_e(\phi) = \int_\Omega \left(F_c(\phi) + \frac{\epsilon^2}{2}|\nabla\phi|^2 \right) d\mathbf{x} - \int_\Omega F_e(\phi)\, d\mathbf{x},$$

where $F_c(\phi) = \frac{\theta}{2}\left[(1+\phi)\ln\left(\frac{1+\phi}{2}\right) + (1-\phi)\ln\left(\frac{1-\phi}{2}\right)\right]$ and $F_e(\phi) = -\frac{\theta_c}{2}(1-\phi^2)$. Treating $\mathcal{E}_c(\phi)$ implicitly and $\mathcal{E}_e(\phi)$ explicitly [8], the following nonlinear convex splitting scheme is obtained:

$$\begin{aligned} \frac{\phi^{n+1} - \phi^n}{\Delta t} &= \Delta\left(\frac{\delta \mathcal{E}_c(\phi^{n+1})}{\delta\phi} - \frac{\delta \mathcal{E}_e(\phi^n)}{\delta\phi} \right) \\ &= \Delta\left(\frac{\theta}{2}\ln\left(\frac{1+\phi^{n+1}}{1-\phi^{n+1}}\right) - \epsilon^2\Delta\phi^{n+1} - \theta_c\phi^n \right). \end{aligned} \tag{4}$$

The nonlinearity in Eq. (4) comes from the term $\ln\left(\frac{1+\phi^{n+1}}{1-\phi^{n+1}}\right)$ and this can be handled using a Newton-type linearization

$$\ln\left(\frac{1+\phi^{n,m+1}}{1-\phi^{n,m+1}}\right) \approx \ln\left(\frac{1+\phi^{n,m}}{1-\phi^{n,m}}\right) + \frac{2}{1-(\phi^{n,m})^2}(\phi^{n,m+1} - \phi^{n,m})$$

for $m = 0, 1, \ldots$. We then develop a Newton-type iterative method as

$$\begin{aligned} &\phi^{n,m+1} - \Delta t\Delta\left(\frac{\theta}{1-(\phi^{n,m})^2}\phi^{n,m+1} - \epsilon^2\Delta\phi^{n,m+1}\right) \\ &= \phi^n + \Delta t\Delta\left[\frac{\theta}{2}\ln\left(\frac{1+\phi^{n,m}}{1-\phi^{n,m}}\right) - \frac{\theta}{1-(\phi^{n,m})^2}\phi^{n,m} - \theta_c\phi^n\right], \end{aligned} \tag{5}$$

where $\phi^{n,0} = \phi^n$, and we set $\phi^{n+1} = \phi^{n,m+1}$ if a relative l_2-norm of the consecutive error $\frac{\left\|\phi^{n,m+1}-\phi^{n,m}\right\|_2}{\left\|\phi^{n,m}\right\|_2}$ is less than a tolerance *tol* (is set to 10^{-8} in this paper).

Equation (5) can be rewritten in the form

$$\mathbf{A}\phi^{n,m+1} = \phi^n + \Delta t\Delta\left[\frac{\theta}{2}\ln\left(\frac{1+\phi^{n,m}}{1-\phi^{n,m}}\right) - \frac{\theta\phi^{n,m}}{1-(\phi^{n,m})^2} - \theta_c\phi^n\right], \tag{6}$$

where

$$\mathbf{A} = 1 + \Delta t\mathcal{F}^{-1}\left(\xi_{k_1}^2 + \xi_{k_2}^2\right)\mathcal{F}\frac{\theta}{1-(\phi^{n,m})^2}1 + \Delta t\epsilon^2\mathcal{F}^{-1}\left(\xi_{k_1}^2 + \xi_{k_2}^2\right)^2\mathcal{F},$$

where $\mathcal{F}$ denotes the discrete Fourier transform and $\mathcal{F}^{-1}$ its inverse transform. In this paper, the biconjugate gradient (BICG) method is used to solve the system (6) and the stopping criterion for the BICG iteration is that the relative residual norm is less than *tol* (is set to 10^{-8} in this paper).

3. Numerical experiments

3.1. Relation between the ϵ value and the thickness of the interfacial layer

For a polynomial free energy $\frac{1}{4}(\phi^2-1)^2$, the equilibrium states are -1 and 1, and ϕ varies from -0.9 to 0.9 over a distance of about $2\sqrt{2}\epsilon\tanh^{-1}(0.9)$. Thus, it is well known that if we want this value to be about m grid points, then $\epsilon_m = \frac{hm}{2\sqrt{2}\tanh^{-1}(0.9)}$. This formula was verified in previous works [6,12,15,19]. However, for the logarithmic free energy $F(\phi)$ in (3), the equilibrium states depend on the absolute temperature θ, thus, ϵ also depends on θ. For this case, there is no known formula to the authors' knowledge. In this section, we derive a useful formula for the relation between the ϵ value and the thickness of the interfacial layer for $F(\phi)$. Let ϕ^{eq} be a positive equilibrium state for $F(\phi)$ with given θ and θ_c, i.e., $F'(-\phi^{eq}) = F'(\phi^{eq}) = 0$. Figure 2 shows ϕ^{eq} for various θ with $\theta_c = 1$.

In order to see the relation between the ϵ value and the thickness of the interfacial layer, we take the initial condition as

$$\phi(x,0) = \begin{cases} 0.8 & \text{if } |x-2| < 1, \\ -0.8 & \text{otherwise} \end{cases}$$

on $\Omega = [0,4]$. Here, we use $h = 4/100$, $\Delta t = 0.001$, and $\theta_c = 1$, and define an equilibrium state as an state when the discrete l_2-norm of the difference

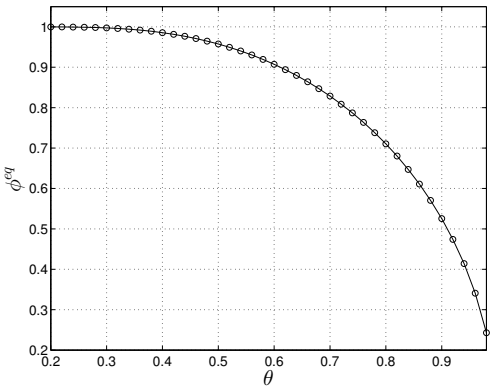

θ	0.3	0.4	0.6	0.7	0.8	0.9
ϕ^{eq} ($\approx$)	0.9974	0.9856	0.9073	0.8286	0.7104	0.5254

FIGURE 2. ϕ^{eq} for various θ with $\theta_c = 1$.

between ϕ^{n+1} and ϕ^n becomes less than 10^{-6}. Figures 3(a) and (b) show the interfacial layer at the equilibrium state for various θ with $\epsilon = 0.5h$ and $\epsilon = h$, respectively. Table 1 lists the numbers of grid points in the interfacial layer (from $\phi = -0.9\phi^{eq}$ to $\phi = 0.9\phi^{eq}$). The results in Fig. 3 and Table 1 indicate that ϵ depends not only on m, which is the number of grid points, but also on θ.

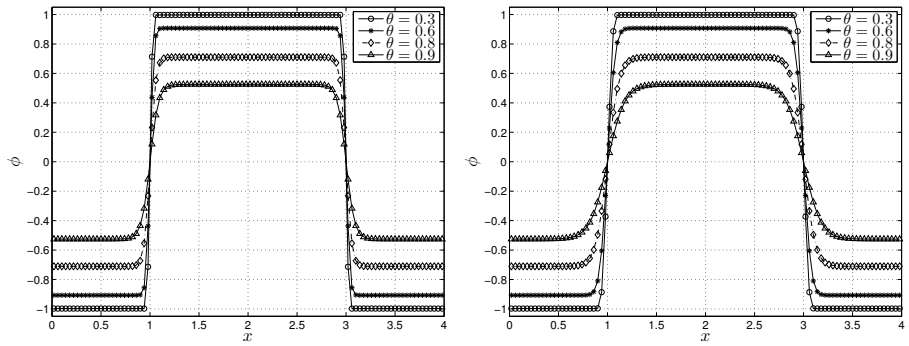

(a) (b)

FIGURE 3. Interfacial layer at the equilibrium state for various θ with (a) $\epsilon = 0.5h$ and (b) $\epsilon = h$. Here, $\theta_c = 1$ is used.

TABLE 1. Numbers of grid points in the interfacial layer (from $\phi = -0.9\phi^{eq}$ to $\phi = 0.9\phi^{eq}$).

θ	0.3	0.4	0.6	0.7	0.8	0.9
$\epsilon = 0.5h$	2	2	2	4	4	6
$\epsilon = h$	4	4	6	6	8	12
$\epsilon = 1.5h$	4	6	8	10	12	18

Using the data in Table 1 and the **fit** command in MATLAB [14], we derive a fitting polynomial surface of degree 2 in θ and m:

$$\epsilon(\theta, m) = \frac{h}{10}(4.835\theta^2 - 3.752\theta m + 0.005m^2 - 4.01\theta + 4.078m + 0.693). \tag{7}$$

Figure 4 shows the polynomial surface (7) and the data (open circles) in Table 1. Equation (7) is a useful formula because if we have the θ value and want m grid points to lie in the interfacial layer, it gives us an approximate value of ϵ. Note that we can increase the highest degrees of the polynomial. For convenience of exposition, we limit them to 2. Figure 5 shows the evolution of $\phi(x, t)$ with $\epsilon(\theta, 8)$ for various θ. It is observed that 8 grid points lie in the interfacial layer (from $\phi = -0.9\phi^{eq}$ to $\phi = 0.9\phi^{eq}$, this range is marked with horizontal dashed lines).

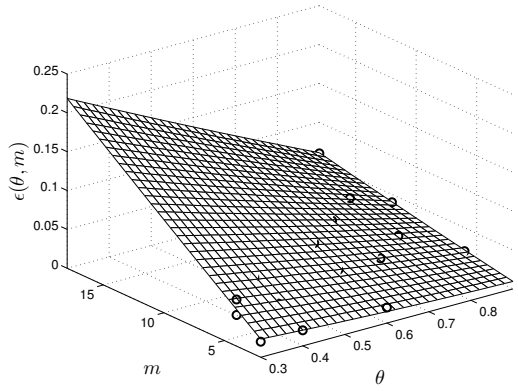

FIGURE 4. Surface fitting: $\epsilon(\theta, m) = 0.1h(4.835\theta^2 - 3.752\theta m + 0.005m^2 - 4.01\theta + 4.078m + 0.693)$.

3.2. Comparison with a linear convex splitting scheme

For a simple implementation, a linear convex splitting scheme was coupled with the Fourier spectral method for the CH equation in [11]. The linear scheme

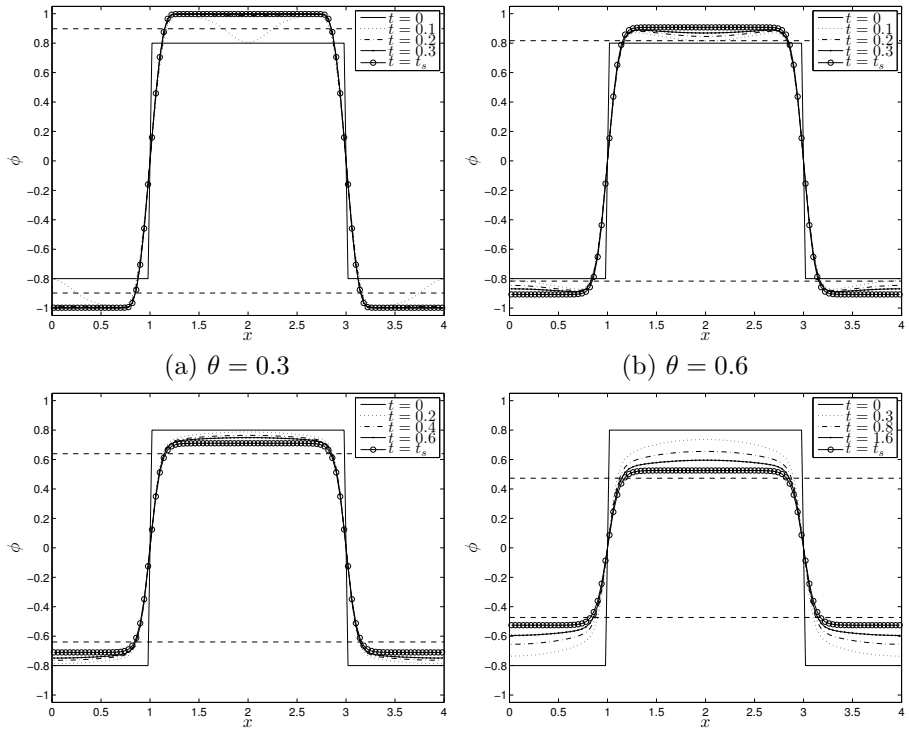

(a) $\theta = 0.3$ (b) $\theta = 0.6$

(c) $\theta = 0.8$ (d) $\theta = 0.9$

FIGURE 5. Evolution of $\phi(x,t)$ with $\epsilon(\theta, 8)$ for various θ. In each subfigure, horizontal dashed lines represent the range from $\phi = -0.9\phi^{eq}$ to $\phi = 0.9\phi^{eq}$.

is based on the following splitting:

$$\begin{aligned} & F(\phi) \\ &= F_c(\phi) - F_e(\phi) \\ &= \frac{s}{2}\phi^2 - \left[-\frac{\theta}{2}\left((1+\phi)\ln\left(\frac{1+\phi}{2}\right) + (1-\phi)\ln\left(\frac{1-\phi}{2}\right)\right) - \frac{\theta_c}{2}(1-\phi^2) + \frac{s}{2}\phi^2 \right], \end{aligned}$$

where $s > 0$ is the splitting parameter. For $F_e(\phi)$ to be convex, it requires that $F_e''(\phi) = s - C(\theta, \phi) \geq 0$, i.e., $s \geq C(\theta, \phi)$, where

$$C(\theta, \phi) = \frac{\theta}{1-\phi^2} - \theta_c.$$

Figure 6 shows $C(\theta, \phi^{eq})$ for various θ with $\theta_c = 1$.

There is no maximum principle for the CH equation. However, from the numerical experiments, the minimum and maximum values of ϕ are in the

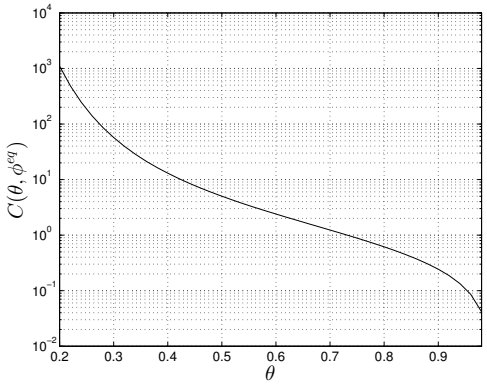

FIGURE 6. $C(\theta, \phi^{eq})$ for various θ with $\theta_c = 1$.

neighborhood of the equilibrium states, $-\phi^{eq}$ and ϕ^{eq}. And we need to take the value of s as small as possible to minimize the local discretization error [8]. Thus, it is reasonable to choose the value of s based on ϕ^{eq} as follows:

$$s = C(\theta, \psi), \tag{8}$$

where $\psi = \min[0.5(1+\phi^{eq}), 1.1\phi^{eq}]$ and 1.1 is a safety factor. Using the formula (8) for the splitting parameter, we can avoid trial and error approach to find an appropriate splitting parameter, which makes $F_e(\phi)$ be convex and minimizes the local discretization error depending on the safety factor. Table 2 lists the values of s for various θ with $\theta_c = 1$.

TABLE 2. Values of s for various θ with $\theta_c = 1$.

θ	0.3	0.4	0.6	0.7	0.8	0.9
$s = C(\theta, \psi)$	115.0843	26.9245	5.6283	3.1378	1.0548	0.3515

We now consider the phase separation using the linear and nonlinear schemes. The initial condition is $\phi(x, y, 0) = \text{rand}(x, y)$ on $\Omega = [0, 100] \times [0, 100]$, where $\text{rand}(x, y)$ is a random number between -0.05 and 0.05, and $h = \Delta t = 1$, $\theta = 0.8$, $\theta_c = 1$, and $\epsilon = \epsilon(\theta, 8)$ are used. Figures 7(a) and (b) show the evolution of $\phi(x, y, t)$ using the linear scheme with $s = 1.0548$ and 115.0843, respectively. As mentioned in Table 2, the appropriate value of s for $\theta = 0.8$ is 1.0548. Thus, we observe that the linear scheme with $s = 1.0548$ reasonably reveals the dynamics of morphology, whereas the linear scheme with $s = 115.0843$ leads to incorrect morphologies in the phase separation process. Figure 7(c) shows the evolution of $\phi(x, y, t)$ using the nonlinear scheme, which is same as that in Fig. 7(a).

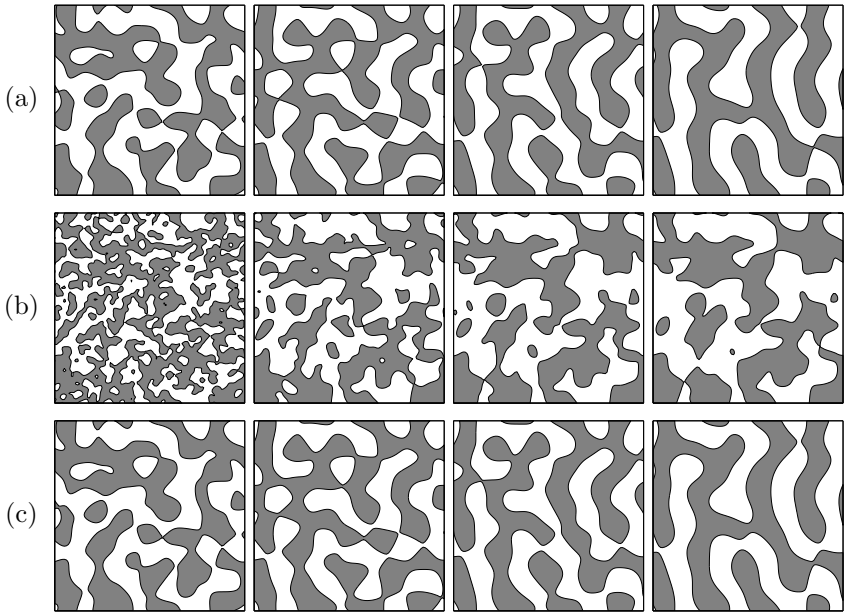

FIGURE 7. Evolution of $\phi(x, y, t)$ using (a) the linear scheme with $s = 1.0548$, (b) the linear scheme with $s = 115.0843$, and (c) the nonlinear scheme. Here, $\theta = 0.8$, $\theta_c = 1$, and $\epsilon = \epsilon(\theta, 8)$ are used. The times are $t = 100$, 400, 700, and 1000 (from left to right).

3.3. Effect of an average concentration

We examine the evolution from random nonequilibrium states with different average concentrations. The initial condition is $\phi(x, y, 0) = \bar{\phi} + \text{rand}(x, y)$ on $\Omega = [0, 200] \times [0, 200]$, and $h = \Delta t = 1$, $\theta = 0.8$, $\theta_c = 1$, and $\epsilon(\theta, 8)$ are used. Figures 8 and 9 show the evolution of $\phi(x, y, t)$ with $\bar{\phi} = -0.3$ and 0, respectively. Depending on the value of $\bar{\phi}$, we have different patterns. Figure 10 shows the evolution of the energy with $\bar{\phi} = -0.3$ and 0. We observe that all the energy curves are nonincreasing in time.

4. Conclusion

In this paper, we presented the nonlinear convex splitting Fourier spectral scheme for the CH equation with the logarithmic free energy, which is an appropriate extension of Eyre's idea of convex-concave decomposition of the energy functional. Using the nonlinear scheme, we derived the useful formula for the relation between the ϵ value and the thickness of the interfacial layer. And we observed through numerical simulations that an inappropriate value of the splitting parameter of the linear scheme leads to incorrect morphologies in the

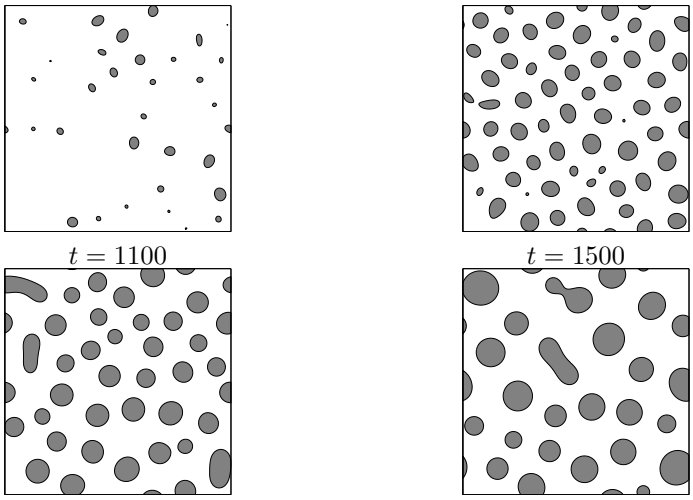

FIGURE 8. Evolution of $\phi(x, y, t)$ with $\bar{\phi} = -0.3$. Here, $\theta = 0.8$, $\theta_c = 1$, and $\epsilon = \epsilon(\theta, 8)$ are used. The times are shown below each subfigure.

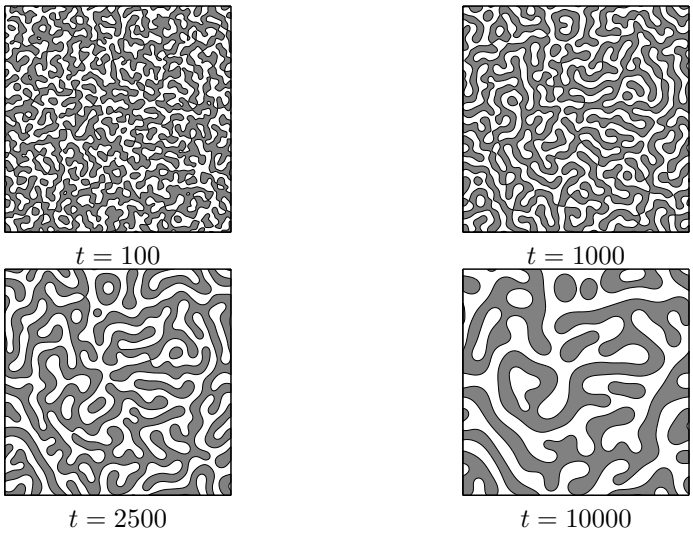

FIGURE 9. Evolution of $\phi(x, y, t)$ with $\bar{\phi} = 0$. Here, $\theta = 0.8$, $\theta_c = 1$, and $\epsilon = \epsilon(\theta, 8)$ are used. The times are shown below each subfigure.

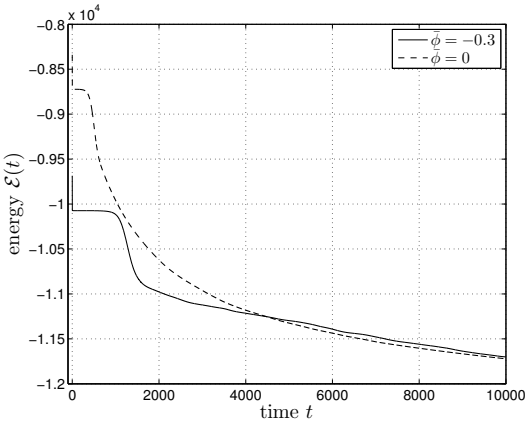

FIGURE 10. Evolution of the energy with $\bar{\phi} = -0.3$ and 0.

phase separation process, whereas the nonlinear scheme reasonably reveals the dynamics of morphology. As a future research direction, it would be interesting to compare the dynamics of morphology using the CH equation with the logarithmic free energy with real experimental data.

Acknowledgment. The authors thank the reviewers for the constructive and helpful comments on the revision of this article.

References

[1] J. T. Cabral, J. S. Higgins, T. C. B. McLeish, S. Strausser, and S. N. Magonov, *Bulk spinodal decomposition studied by atomic force microscopy and light scattering*, Macromolecules **34** (2001), 3748–3756.

[2] J. W. Cahn, *On spinodal decomposition*, Acta Metall. **9** (1961), 795–801.

[3] J. W. Cahn and J. E. Hilliard, *Free energy of a nonuniform system. I. Interfacial free energy*, J. Chem. Phys. **28** (1958), 258–267.

[4] L. Q. Chen and J. Shen, *Applications of semi-implicit Fourier-spectral method to phase field equations*, Comput. Phys. Commun. **108** (1998), 147–158.

[5] M. Cheng and A. D. Rutenberg, *Maximally fast coarsening algorithms*, Phys. Rev. E **72** (2005), 055701(R).

[6] J.-W. Choi, H. G. Lee, D. Jeong, and J. Kim, *An unconditionally gradient stable numerical method for solving the Allen-Cahn equation*, Phys. A **388** (2009), no. 9, 1791–1803.

[7] M. I. M. Copetti and C. M. Elliott, *Numerical analysis of the Cahn-Hilliard equation with a logarithmic free energy*, Numer. Math. **63** (1992), no. 1, 39–65.

[8] D. J. Eyre, *Unconditionally gradient stable time marching the Cahn-Hilliard equation*, in Computational and mathematical models of microstructural evolution (San Francisco, CA, 1998), 39–46, Mater. Res. Soc. Sympos. Proc., 529, 1998.

[9] H. Gómez, V. M. Calo, Y. Bazilevs, and T. J. Hughes, *Isogeometric analysis of the Cahn-Hilliard phase-field model*, Comput. Methods Appl. Mech. Engrg. **197** (2008), no. 49-50, 4333–4352.

[10] D. Jeong and J. Kim, *A practical numerical scheme for the ternary Cahn-Hilliard system with a logarithmic free energy*, Phys. A **442** (2016), 510–522.

[11] ———, *Practical estimation of a splitting parameter for a spectral method for the ternary Cahn-Hilliard system with a logarithmic free energy*, Math. Methods Appl. Sci. **40** (2017), no. 5, 1734–1745.
[12] J. Kim, *Phase-field models for multi-component fluid flows*, Commun. Comput. Phys. **12** (2012), no. 3, 613–661.
[13] D. Lee, J.-Y. Huh, D. Jeong, J. Shin, A. Yun, and J. Kim, *Physical, mathematical, and numerical derivations of the Cahn–Hilliard equation*, Comp. Mater. Sci. **81** (2014), 216–225.
[14] The MathWorks, Inc., Natick, MA, USA.
[15] J. Shin, D. Jeong, and J. Kim, *A conservative numerical method for the Cahn-Hilliard equation in complex domains*, J. Comput. Phys. **230** (2011), no. 19, 7441–7455.
[16] J. Shin, S. Kim, D. Lee, and J. Kim, *A parallel multigrid method of the Cahn–Hilliard equation*, Comp. Mater. Sci. **71** (2013), 89–96.
[17] J. Shin, H. G. Lee, and J.-Y. Lee, *Convex Splitting Runge-Kutta methods for phase-field models*, Comput. Math. Appl. **73** (2017), no. 11, 2388–2403.
[18] H. Song, *Energy SSP-IMEX Runge-Kutta methods for the Cahn-Hilliard equation*, J. Comput. Appl. Math. **292** (2016), 576–590.
[19] S. Zhai, Z. Weng, and X. Feng, *Fast explicit operator splitting method and time-step adaptivity for fractional non-local Allen-Cahn model*, Appl. Math. Model. **40** (2016), no. 2, 1315–1324.

Junseok Kim
Department of Mathematics
Korea University
Seoul 02841, Korea
Email address: cfdkim@korea.ac.kr

Hyun Geun Lee
Department of Mathematics
Kwangwoon University
Seoul 01897, Korea
Email address: leeh1@kw.ac.kr